

# Evacuation Vector Field in Crowd Dynamics

Liwen Zhou

School of Mathematics, East China University of Science and Technology, Shanghai, China

Email: 24662240372@qq.com

**How to cite this paper:** Zhou, L.W. (2022)

Evacuation Vector Field in Crowd Dynamics. *Journal of Applied Mathematics and Physics*, 10, 1547-1560.

<https://doi.org/10.4236/jamp.2022.105108>

**Received:** April 2, 2022

**Accepted:** May 15, 2022

**Published:** May 18, 2022

Copyright © 2022 by author(s) and Scientific Research Publishing Inc.

This work is licensed under the Creative Commons Attribution International License (CC BY 4.0).

<http://creativecommons.org/licenses/by/4.0/>



Open Access

---

## Abstract

The geometrical effect is one of the most important factors in the kinetic modeling of crowd evacuation, besides the interaction between agents. More precisely, in the process of crowd evacuation, agents have the desire to reach the exit, and the ability to avoid the walls or obstacles. In this study, we propose the *evacuation vector field* which incorporates the geometrical effects in crowd evacuation. This is useful for modeling the crowd evacuation from complex venue.

## Keywords

Kinetic Models, Crowd Evacuation, Evacuation Vector Field

---

## 1. Introduction

The study of crowd dynamics of multi-agent system has wide applications in engineering and social sciences. Researchers have been attracted by both analytical challenges and computational problems generated by the complexity features of these models. The modeling of crowd dynamics can be developed at different scales, ranging from micro-scale, meso-scale to macro-scale [1] [2] [3] [4] [5]. At the micro-scale, the motion is governed by coupling ordinary differential equations of each agent; in this case, their positions and velocities are identified as dependent variables of time, for example, the social force model used in [6] [7] [8], among others; At the macro-scale, the models by classical conservation equations are utilized, where the multi-agent system is treated as a “thinking fluid”; The state of the system is described by averaged gross quantities such as density, linear momentum and kinetic energy, regarded as dependent variables of time and space [9]-[18]; At the intermediate scale, the system is described by kinetic equations, where the dependent variable is a probability distribution of the micro-state of the agents [1] [2] [5] [19] [20] [21]. Note that in the kinetic modeling of crowd dynamics, both collective strategy and the individual interactions

have to be considered. We also mention that, the kinetic models provide an important link between the micro-scale and macro-scale models.

Crowd evacuation from a bounded domain is a very important topic in crowd dynamics, which has wide applications for example in safety control and crisis managing, see [22] [23] [24] [25] [26] and references therein. In the kinetic model proposed in [1] [2] [19], the agents are viewed as active particles, whose micro-states are defined by their position and velocity direction; the overall state of the system is governed by a distribution function of the micro-states, so evolutionary equation of the distribution function is obtained by a local balance of particles incorporating transport and interactions in a kinetic fashion. Note that the interactions are nonlinearly additive, so a nontrivial global effect is produced, rather than the sum of all the individual interactions. More precisely, there are several factors to be considered in crowd evacuation, including: firstly, due to *geometrical effects*, agents have the desire to reach the exits and the ability to avoid the walls or obstacles; secondly, in the process of *interactions between agents*, agents have the tendency to search for less crowded moving directions, and the trend to follow the main stream of the motion.

In the current study, we will investigate the crowd dynamics in more complex domain, in which there are interior walls and doors that divide the domain into several chambers, beside walls and exits on the boundary. For more complex domain, we emphasize that the geometrical effects may come from the walls both inside the domain and on the boundary, the exits, and the doors connecting the chambers. These geometrical properties are incorporated in the geometrical preferred direction which is specified such that an agent can avoid the wall and approach the exit through the *evacuation vector* defined with respect to its position. This vector field depends only on the geometry of the domain, thus independent of time. It will be useful for modeling the crowd evacuation from complex venue by specifying the corresponding evacuation vector field.

We also mention that there are various other applications of the crowd dynamics, such as vehicular traffic [27] [28], particle swarm [29], migration phenomena on networks [30], coupling between pedestrian movement with traffic flow or social interaction [31] [32] [33] [34], and others, see the recent books [35] [36] for the state of the art progress, challenges and future research perspectives in the area of modeling and simulation of crowd dynamics.

## 2. The Model and the Evacuation Vector Field

Follow the notations in [2] [19], let  $\Sigma \subset \mathbb{R}^2$  denote a bounded domain, with boundary  $\partial\Sigma$  including exits and walls. For instance, beside walls and exits on the boundary, we assume that there are interior walls and doors inside the domain that they separate the domain into several chambers, as shown in **Figure 1**. The key geometrical property of the domain is that, there are *exits* on the boundary, *doors* inside the domain, and *walls* both on the boundary and inside the domain.

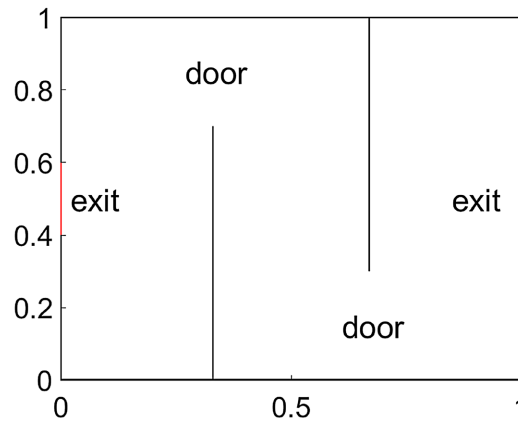


**Figure 1.** Geometry of a bounded domain with *exits* on the boundary, *doors* inside the domain, and *walls* both on the boundary and inside the domain.

We consider a multi-agent system with  $J$  species. For  $j=1, \dots, J$ , we denote  $f^j = f^j(t, x, y)$  the distribution function of  $j$ -th species at time  $t \geq 0$ ,  $(x, y) \in \Sigma$ ,  $\mathbf{v} \in \theta_v$ . Here  $(x, y) \in \Sigma$  denote position and  $\mathbf{v} = v(\cos \theta, \sin \theta) \in \theta_v$  denote velocity, where  $v$  is the velocity modulus,  $\theta$  is the velocity direction, and  $\theta_v \in \mathbb{R}^2$  is the velocity domain. Since polar coordinates for the velocity is used, the distribution function can also be written as  $f^j = f^j(t, x, y, v, \theta)$ . Motivated by the granularity of crowd dynamics when the crowd size is not enough to justify the continuity of the distribution function over the variable  $\theta$ , following [2] [19], we assume that the variable  $\theta$  is discrete that can take values in the set:

$$I_\theta = \left\{ \theta_i = \frac{i-1}{N_d} 2\pi : i = 1, \dots, N_d \right\}, \quad (2.1)$$

where  $N_d$  is the maximum number of possible directions. Next, the velocity modulus  $v$  is modeled as a continuous deterministic variable which evolves in time and space according to macroscopic effects determined by the overall dynamics. In fact, experimental studies show that in practical situations the speed of pedestrians depends mainly on the level of congestion around them, this means that the velocity modulus  $v$  depends formally on the local density. Since the variable  $v$  is determined by local density, the kinetic type representation is given by the reduced distribution function

$$f^j(t, x, y, \theta) = \sum_{i=1}^{N_d} f_i^j(t, x, y) \delta(\theta - \theta_i), \quad (2.2)$$

where  $f_i^j(t, x, y) = f^j(t, x, y, \theta_i)$  represents the distribution density of  $j$ -th species at time  $t$  and position  $x, y$ , move with direction  $\theta_i$ . Here  $\delta$  denotes the Dirac delta function. As in [19], dimensionless quantities are used. That is, we set reference quantities:  $L$ , the characteristic length of the domain;  $V_M$ , the highest velocity modulus that an agent can reach in low density and perfect environmental conditions;  $T$ , reference time, given by  $L/V_M$ ;  $\rho_M$ , the maximal admissible number of agents per unit area. Then, the dimensionless position

$(\hat{x}, \hat{y}) = (x/L, y/L)$ , dimensionless time  $\hat{t} = t/T$ , dimensionless velocity modulus  $\hat{v} = v/V_M$ , and dimensionless distribution function  $\hat{f} = f/M$  will be used, although hats will be omitted for simplicity. The local density of  $j$ -th species can be obtained by summing the distribution functions over the set of directions:

$$\rho^j(t, x, y) = \sum_{i=1}^{N_d} f_i^j(t, x, y), \tag{2.3}$$

and the total local density is

$$\rho(t, x, y) = \sum_{j=1}^J \rho^j(t, x, y) = \sum_{j=1}^J \sum_{i=1}^{N_d} f_i^j(t, x, y), \tag{2.4}$$

then, similar to one species dynamics considered in [2] [19], for each  $i = 1, 2, \dots, N_d$ ,  $j = 1, 2, \dots, J$ , the local balance of agents can be given by

$$\frac{\partial f_i^j}{\partial t} + \nabla \cdot (\mathbf{V}_i^j[\rho](t, x, y) f_i^j(t, x, y)) = \mathcal{J}_i^j[f](t, x, y), \tag{2.5}$$

where  $\mathcal{J}_i^j[f]$  on the right hand side is the collisional term representing the net balance of particles that move with direction  $\theta_i$ , due to geometrical effects and interactions between agents, which will be specified in next two subsections, and

$$\mathbf{V}_i^j[\rho](t, x, y) = \phi^j[\rho](t, x, y)(\cos \theta_i, \sin \theta_i) \tag{2.6}$$

is the transport coefficient indicating the transport velocity of  $j$ -th species along direction  $\theta_i$ , with *velocity modulus* specified by  $\phi^j[\rho](t, x, y)$ . Here the square brackets are used to denote that  $\phi^j$  depends on  $\rho$  in a functional way, for instance, it can depend on  $\rho$  as studied in [37], or on the gradient of  $\rho$  by using the concept of perceived density [38]. For simplicity, we follow [37], that the maximal speed is kept under low density conditions (free flow regime), up to a certain critical density  $\rho_c$ , the velocity modulus decreases to zero (slowdown zone) for values of  $\rho$  greater than  $\rho_c$ . In the slowdown zone, a polynomial-type dependence of the velocity modulus on the local density is used. In this study, we take  $\rho_c = 1/5$ , the functional  $\phi^j[\rho]$  is taken as

$$\phi^j(\rho) = \begin{cases} 1, & 0 \leq \rho < 1/5, \\ 125/32 * (\rho - 1) * (\rho^2 - 4/5 \rho - 1/5), & 1/5 \leq \rho \leq 1. \end{cases} \tag{2.7}$$

To model the collision term on the right hand side of (2.5), we introduce the *evacuation vector field*. Follow [2] [19], we use the notion of *test particles*, with state  $(x, y, \theta_i)$  representing any agent in the whole system; *candidate particles*, with state  $(x, y, \theta_h)$ , which can reach in probability the state of the test particles after individual-based interactions with the environment or with field particles; and *field particles*, with state  $(x, y, \theta_k)$ , whose presence triggers the interactions of the candidate particles. The geometrical effects include:

1) *The desire to reach the exit*. In the crowd evacuation, the first rule in the dynamics is the desire to reach the exit. Recall that for a simple domain considered in [19], given a candidate particle at the point  $(x, y)$ , then the goal to reach the exit is determined by two factors, first, its distance to the exit, and

second, a unit vector pointing from  $(x, y)$  to the exit. For the present case of complex domain with interior walls (or obstacles), these two factors should be modified. Since the domain is separated into several chambers, each agent at  $(x, y)$  should find the correct door or exit, called *escaping exit* (EE) for  $(x, y)$ , to escape from the current chamber, till finally reach the exit. Then the distance from  $(x, y)$  to its escaping exit is defined as

$$d_{EE}(x, y) = \min_{(\bar{x}, \bar{y}) \in EE} \sqrt{(x - \bar{x})^2 + (y - \bar{y})^2}, \quad (2.8)$$

and the unit vector  $\mathbf{u}_{EE}(x, y)$ , called *evacuation vector*, is defined pointing from  $(x, y)$  to the escaping exit. See **Figure 2(a)** for illustration of  $d_{EE}(x, y)$  and  $\mathbf{u}_{EE}(x, y)$ , **Figure 2(b)** for illustration of an evacuation vector field. Note that we slightly modified this vector field near the top of the first chamber and the bottom of the second chamber to better avoid the wall, by taking the vector pointing to the midpoint of the door.

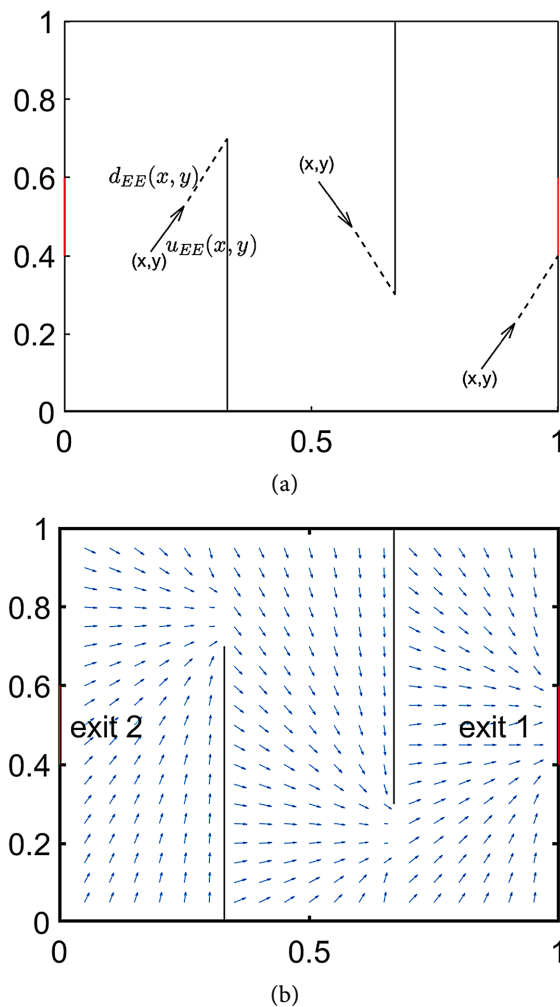


**Figure 2.** (a) The distance from  $(x, y)$  to its *escaping exit* (EE) is denoted by  $d_{EE}(x, y)$ , and the unit vector pointing from  $(x, y)$  to the escaping exit is denoted by  $\mathbf{u}_{EE}(x, y)$ . (b) The evacuation vector field for species aiming for Exit 1 on the right boundary.

2) *The ability to avoid the wall.* The second rule in the dynamics is the ability to avoid the wall. As in [19], given a candidate particle at the point  $(x, y)$  moving with direction  $\theta_h$ , we define the distance  $d_w(x, y, \theta_h)$  from the particle to a wall at a point  $(x_w, y_w)$  where the particle is expected to collide with the wall. Then select the unit tangent vector  $\mathbf{u}_w(x, y, \theta_h)$  to the wall at  $(x_w, y_w)$  pointing to the direction much closer to the evacuation exit. See Figure 3 for illustration of  $(x_w, y_w)$  and  $\mathbf{u}_w(x, y, \theta_h)$ . This direction will be used to construct a geometrical preferred direction avoiding a collision with the walls.

By taking into account both factors described above, one has the *geometrical preferred direction*  $\theta_G$  defined by

$$\begin{aligned} \mathbf{u}_G(x, y, \theta_h) &= \frac{(1 - d_{EE}(x, y))\mathbf{u}_{EE}(x, y) + (1 - d_w(x, y, \theta_h))\mathbf{u}_w(x, y, \theta_h)}{\|(1 - d_{EE}(x, y))\mathbf{u}_{EE}(x, y) + (1 - d_w(x, y, \theta_h))\mathbf{u}_w(x, y, \theta_h)\|} \\ &:= (\cos \theta_G, \sin \theta_G). \end{aligned} \tag{2.9}$$

Note that this choice means, the direction  $\mathbf{u}_{EE}$  (resp.,  $\mathbf{u}_w$ ) is more weighted while the agent is closer to the escaping exit (resp., wall).

To complete the model, we next consider the interactions between agents, by incorporating the tendency to search for less crowded directions, and the trend to follow the main stream of the motion, then the *interaction-based preferred direction*  $\theta_p$  is defined through the vector

$$\mathbf{u}_p(\theta_h, \theta_k, \rho) = \frac{\varepsilon \mathbf{u}_F + (1 - \varepsilon)\mathbf{u}_C(\theta_h, \rho)}{\|\varepsilon \mathbf{u}_F + (1 - \varepsilon)\mathbf{u}_C(\theta_h, \rho)\|} := (\cos \theta_p, \sin \theta_p), \tag{2.10}$$

where  $\varepsilon$  is a parameter introduced to measure the compromise of the two factors, the unit vector  $\mathbf{u}_C(\theta_c, \rho) = (\cos \theta_c, \sin \theta_c)$  with direction  $\theta_c$  defined by taking

$$C = \arg \min_{j \in \{h-1, h, h+1\}} \{\partial_j \rho(t, x, y)\}, \tag{2.11}$$

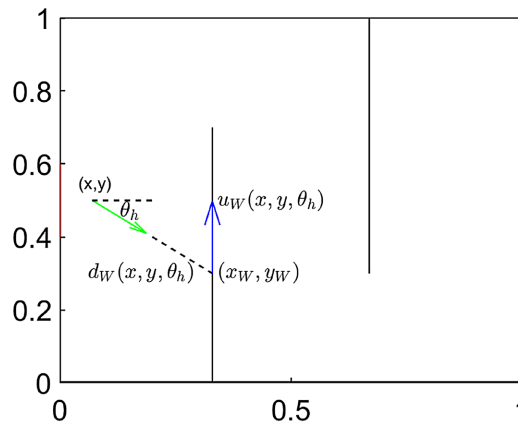


**Figure 3.** A particle in  $(x, y)$  moving with direction  $\theta_h$  is expected to collide the wall at  $(x_w, y_w)$ , with distance  $d_w(x, y, \theta_h)$ .  $\mathbf{u}_w(x, y, \theta_h)$  is the tangent direction to the wall that would take it toward the evacuation exit.

where  $\partial_j \rho$  denotes the directional derivative of  $\rho$  in the direction given by angle  $\theta_j$ .

Now we are ready to specify the collisional term  $\mathcal{J}_i^j[f]$ . First, for the geometrical effects, one introduces  $\mathcal{A}_h^j(i)$  for species  $j$ : the *transition probability* that a candidate particle  $h$ , *i.e.* with direction  $\theta_h$ , of species  $j$ , adjusts its direction into that of the test particle  $\theta_i$  due to the presence of evacuation exit and the wall. A natural constraint for  $\mathcal{A}_h^j(i)$  is

$$\sum_{i=1}^{N_d} \mathcal{A}_h^j(i) = 1 \quad \text{for all } h \in \{1, \dots, N_d\}. \quad (2.12)$$

Consider that an agent changes direction, in probability, only to an adjacent clockwise or counter-clockwise direction in the discrete set  $I_\theta$ , that is, a candidate particle  $h$  may remain in the state  $h$  or turn to the states  $h-1, h+1$ . In the case  $h=1$ , we set  $\theta_{h-1} = \theta_{N_d}$  and, in the case  $h=N_d$ , we set  $\theta_{h+1} = \theta_1$ , due to periodicity of the velocity directions. Then a candidate particle  $h$  will update its direction by choosing the angle closest to  $\theta_G$  defined in (2.9) among the three candidate angles  $\theta_{h-1}, \theta_h$  and  $\theta_{h+1}$ . The transition probability is given by:

$$\mathcal{A}_h^j(i) = \beta_h^j(\alpha) \delta_{s,i} + (1 - \beta_h^j(\alpha)) \delta_{h,i}, \quad i = h-1, h, h+1, \quad (2.13)$$

where

$$s = \arg \min_{j \in \{h-1, h, h+1\}} \{d(\theta_G, \theta_j)\},$$

with

$$d(\theta_p, \theta_q) = \begin{cases} |\theta_p - \theta_q| & \text{if } |\theta_p - \theta_q| \leq \pi, \\ 2\pi - |\theta_p - \theta_q| & \text{if } |\theta_p - \theta_q| > \pi. \end{cases} \quad (2.14)$$

In (2.13),  $\delta$  denotes the Kronecker delta function. The coefficient  $\beta_h^j$  can be assumed proportional to a parameter  $\alpha$ , up to a given constant transition rate  $\bar{\beta}^j$ , thus it is defined by

$$\beta_h^j(\alpha) = \begin{cases} \alpha \bar{\beta}^j & \text{if } d(\theta_h, \theta_G) \geq \Delta\theta, \\ \alpha \bar{\beta}^j \frac{d(\theta_h, \theta_G)}{\Delta\theta} & \text{if } d(\theta_h, \theta_G) < \Delta\theta, \end{cases} \quad (2.15)$$

where  $\Delta\theta = 2\pi/N_d$ , and  $\alpha \in [0, 1]$  is a parameter representing the quality of the domain:  $\alpha = 0$  corresponds to the worst quality which forces agents to slow down or stop, while  $\alpha = 1$  corresponds to the best quality that agents can walk at the desired speed.

Next, for the interaction between agents, one introduces the *transition probability*  $\mathcal{B}_{hk}^{j,\tilde{j}}(i)[\rho]$ , that a candidate particle  $h$ , of species  $j$ , modifies its direction  $\theta_h$  into that of the test particle  $i$ , *i.e.*  $\theta_i$ , due to the search of less congested areas and the interaction with a field particle  $k$  of species  $\tilde{j}$  that moves with direction  $\theta_k$ . For each  $h, k \in \{1, \dots, N_d\}$  and  $j, \tilde{j} \in \{1, \dots, J\}$ , a natural constrain for  $\mathcal{B}_{hk}^{j,\tilde{j}}(i)$  is

$$\sum_{i=1}^{N_d} \mathcal{B}_{hk}^{j,\tilde{j}}(i)[\rho] = 1, \quad (2.16)$$

and the transition probability is given by

$$\mathcal{B}_{hk}^{j,\tilde{j}}(i)[\rho] = \beta_{hk}^{j,\tilde{j}}(\alpha)\rho\delta_{r,i} + (1 - \beta_{hk}^{j,\tilde{j}}(\alpha)\rho)\delta_{h,i}, \quad i = h-1, h, h+1, \quad (2.17)$$

where  $r$  and  $\beta_{hk}^{j,\tilde{j}}$  are defined by:

$$r = \arg \min_{j \in \{h-1, h, h+1\}} \{d(\theta_p, \theta_j)\},$$

$$\beta_{hk}^{j,\tilde{j}}(\alpha) = \bar{\beta}^{j,\tilde{j}} \times \begin{cases} \alpha & \text{if } d(\theta_h, \theta_p) \geq \Delta\theta, \\ \alpha \frac{d(\theta_h, \theta_p)}{\Delta\theta} & \text{if } d(\theta_h, \theta_p) < \Delta\theta, \end{cases} \quad (2.18)$$

in which  $\bar{\beta}^{j,\tilde{j}}$  is the interaction strength between species  $j$  and species  $\tilde{j}$ . Now the collisional term  $\mathcal{J}_i^j[f]$  in the kinetic Equation (2.5) can be specified thus (2.5) becomes

$$\begin{aligned} \frac{\partial f_i^j}{\partial t} + \nabla \cdot (\mathbf{V}_i^j[\rho](t, x, y) f_i^j(t, x, y)) &= \mathcal{J}_{i,G}^j[f](t, x, y) + \mathcal{J}_{i,P}^j[f](t, x, y) \\ &= \mu^j[\rho] \left( \sum_{h=1}^n \mathcal{A}_h^j(i) f_h^j(t, x, y) - f_i^j(t, x, y) \right) \\ &\quad + \eta^j[\rho] \left( \sum_{j=1}^J \sum_{h,k=1}^n \mathcal{B}_{hk}^{j,\tilde{j}}(i)[\rho] f_h^j(t, x, y) f_k^{\tilde{j}}(t, x, y) - f_i^j(t, x, y) \rho(t, x, y) \right), \end{aligned} \quad (2.19)$$

in which  $\mu^j[\rho]$  and  $\eta^j[\rho]$  are interaction rates.

### 3. Numerical Test

In this section, we perform a numerical simulation of crowd evacuation from the complex domain as illustrated in **Figure 1**. For simplicity, we only consider the crowd consists of agents with 2 species, and make species 1 and species 2 move in directions  $N_d = 3$  and  $N_d = 7$ , respectively. In the numerical tests, the side length of the square domain is normalized to be 1, and we take the best quality of the domain that agents can walk at the desired speed thus  $\alpha = 1$ . Some other parameters used in our simulation are: the transition rate due to geometrical effects  $\bar{\beta}^j = 1$  in (2.15), the interaction strength  $\bar{\beta}^{j,\tilde{j}} = \delta_{j,\tilde{j}}$  in (2.18), that is, an agent only follows other agents of the same species, the interaction rates  $\mu^j[\rho] = (1 - \rho)$  and  $\eta^j[\rho] = \rho$  are used in (2.19). Those parameters can be tuned to incorporate more complicated scenarios of interaction between different species and geometrical properties of the domain. Note that only normalized parameters are used in the tests, thus the model can be used for modeling different types of multi-agent system with specific characteristic length, time or speed.

In this test, the square domain is separated into three chambers arranged from left to right, with equal width being 1/3. For simplicity, we ignore the width of the wall. The length of the door connecting two adjacent chambers is set as 0.3, the first door located near the top between the first two chambers, and the second door located near the bottom between the last two chambers. Let species 1 located in the left chamber aiming for exit 1 located on the middle right bound-

dary of the domain, and species 2 located in the right chamber aiming for exit 2 located on the middle left boundary of the domain. The evacuation vector field as discussed above can be adapted for each species, as illustrated in **Figure 4**.

Consider species 1 and species 2 with mass ratio 2:3. Assume that initially species 1 and species 2 are uniformly distributed in  $D_1 = [0.1, 0.2] \times [0.2, 0.35]$  and  $D_2 = [0.8, 0.9] \times [0.65, 0.8]$ , respectively, with equal distribution for each moving direction  $\theta_i, i = 1, \dots, 8$ , that is, the initial distribution is given, for  $i = 1, \dots, 8$ ,

$$f_i^1(0, x, y) = \frac{0.4}{8 * m(D_1 \cup D_2)} \chi_{D_i}(x, y),$$

$$f_i^2(0, x, y) = \frac{0.6}{8 * m(D_1 \cup D_2)} \chi_{D_i}(x, y),$$

in which  $\chi_D$  is the characteristic function of  $D$ ,  $m(D)$  is the area of  $D$ . Note that with this distribution function, the total mass is normalized to be 1. Simulations are obtained by solving the kinetic Equations (2.19) with this initial distribution, while boundary conditions are implicitly imposed by the non-local action over the particles given by the interaction term. Indeed, agents are induced

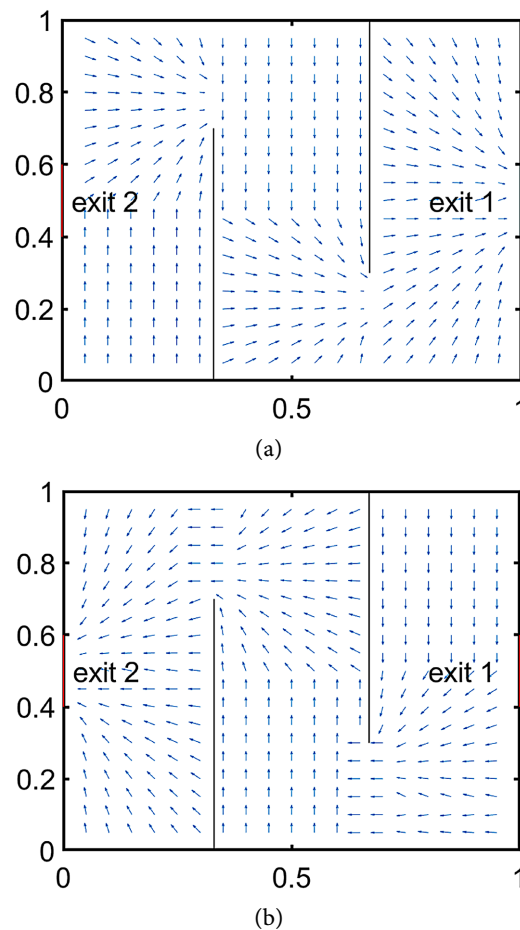


**Figure 4.** (a) Evacuation vector field for species 1 aiming for Exit 1. (b) Evacuation vector field for species 2 aiming for Exit 2.

to avoid walls through the effect of evacuation vector  $EE(x, y)$  pointing from  $(x, y)$  to the escaping exit, and wall-avoiding vector  $W(x, y, \theta_h)$  tangent to the wall at  $(x_w, y_w)$  pointing to the direction more closer to the evacuation exit. Note that even in the extreme case of an agent reaching a point on the wall, the geometrical preferred direction (2.9) induces the agent to move with direction tangent to the wall. The kinetic Equations (2.19) are solved by splitting method, that is, in each time step, the distribution is first updated by the collision, followed by solving a transport equation with first order upwind difference scheme, see [2] [39] for details.

The time evolution of the local density function  $\rho^j(t, x, y)$  for each species  $j$ ,  $j = 1, 2$ , is shown in **Figure 5**, with species 1 in green and species 2 in red, by taking “the size of the exit” = 0.2.

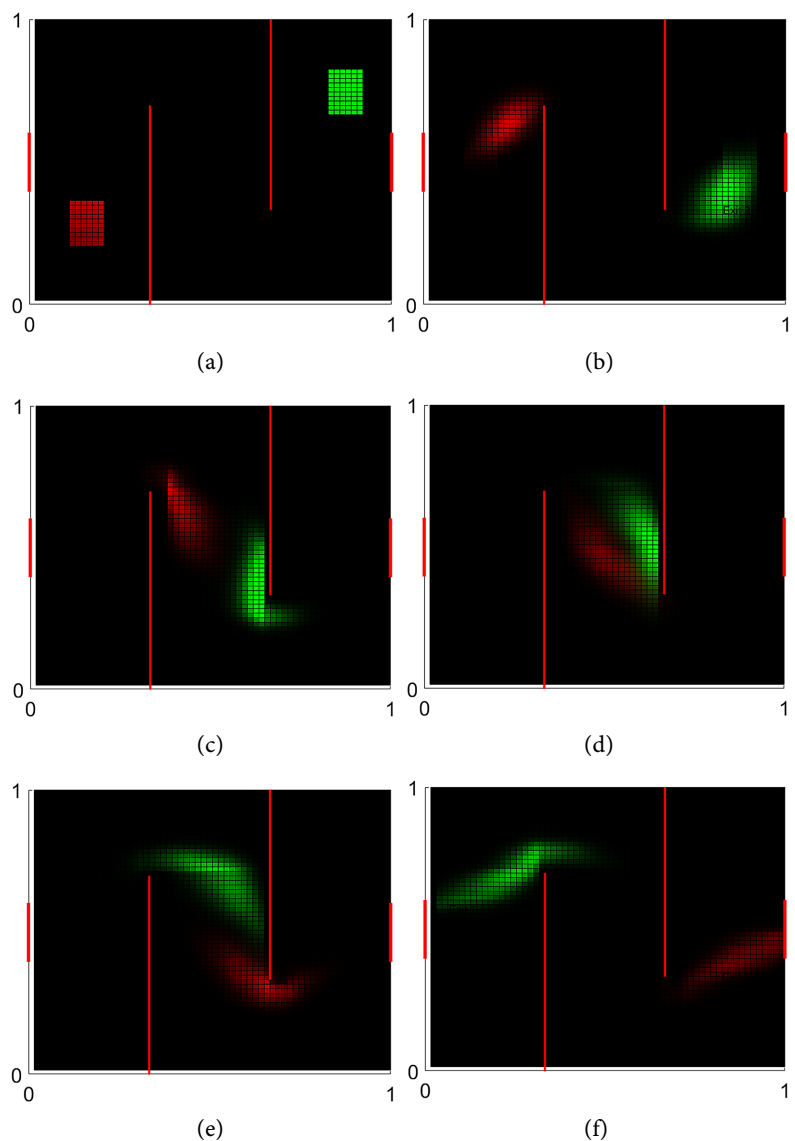
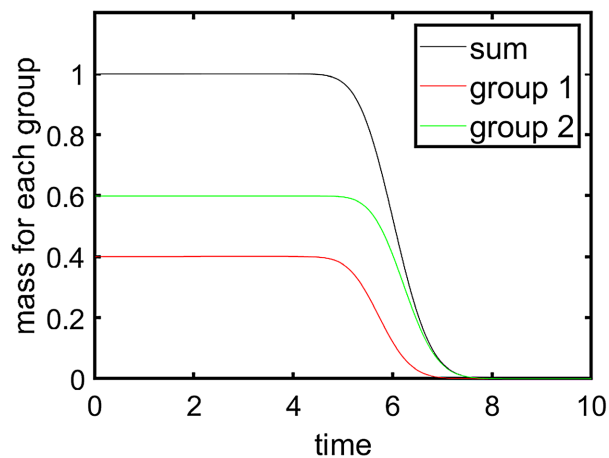


**Figure 5.** The snapshot of the local density distribution functions, with species 1 in green and species 2 in red. (a)  $t = 0$  s; (b)  $t = 1$  s; (c)  $t = 2$  s; (d)  $t = 2.5$  s; (e)  $t = 3$  s; (f)  $t = 4$  s.

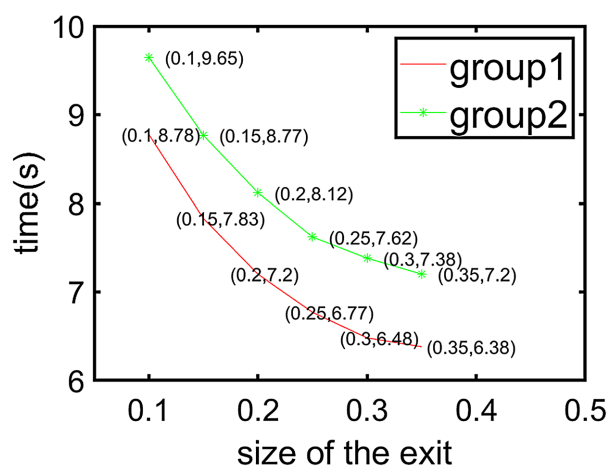
**Figure 6(a)** shows that, the total “mass” for each species, the spatial integration of local density over  $\Sigma$ , is conserved before agents start leaving the domain. The total mass then decreases as agents evacuating the domain. We assume that all agents were evacuated at some time if the local density function is less than  $10^{-8}$  for all  $(x, y) \in \Sigma$  after this time, thus refer this time as evacuation time.

**Figure 6(a)** shows the time evolution of the mass for species 1, 2 and their summation in this setting. We noticed that species 1 starts to leave the domain earlier than species 2, with faster evacuation speed. This is reasonable since species 1 has less density than species 2. We also noticed that the two species are well separated in the motion, since we assumed that the agents only follow others of the same species in the interaction rules.

To further illustrate the relationship between the evacuation time and the size of the exit, we vary the size of the exit in the range  $[0.1, 0.4]$ . The evacuation time is decreased as we increase the size the exit, as shown in **Figure 6(b)**.



(a)



(b)

**Figure 6.** (a) The evolution in time of the mass for species 1, 2 and their summation, with “size of the exit” = 0.2. (b) Evacuation time for different sizes of the exit. (a) Total mass inside the domain; (b) Evacuation time.

## 4. Conclusion and Perspectives

This paper is devoted to introducing the *evacuation vector field* for a kinetic modeling of crowd evacuation in complex domain, in which interior walls and doors divide the domain into several chambers. The geometrical effects may come from the walls both inside the domain and on the boundary, the exits, and the doors connecting the chambers. The *evacuation vector field* incorporated all the geometrical effects in crowd evacuation. This is useful for modeling the crowd evacuation from complex venue. It will be useful for modeling the crowd evacuation from complex venue by specifying the corresponding evacuation vector field.

## Acknowledgements

This research is partially support by National Natural Science Foundation of China (Nos. 11871335 and 11971008).

## Conflicts of Interest

The author declares no conflicts of interest regarding the publication of this paper.

## References

- [1] Bellomo, N. and Bellouquid, A. (2011) On the Modeling of Crowd Dynamics: Looking at the Beautiful Shapes of Swarms. *Networks and Heterogeneous Media*, **6**, 383-399. <https://doi.org/10.3934/nhm.2011.6.383>
- [2] Bellomo, N., Bellouquid, A. and Knopoff, D. (2013) From the Micro-Scale to Collective Crowd Dynamics. *Multiscale Modeling & Simulation*, **11**, 943-963. <https://doi.org/10.1137/130904569>
- [3] Bellomo, N., Piccoli, B. and Tosin, A. (2012) Modeling Crowd Dynamics from a Complex System View Point. *Mathematical Models and Methods in Applied Sciences*, **22**, Article ID: 1230004. <https://doi.org/10.1142/S0218202512300049>
- [4] Carrillo, J.A., Fornasier, M., Toscani, G. and Vecil, F. (2010) Particle, Kinetic, and Hydrodynamic Models of Swarming. In: Naldi, G., Pareschi, L. and Toscani, G., Eds., *Mathematical Modeling of Collective Behavior in Socio-Economic and Life Sciences*, Birkhäuser, Boston, 297-336. [https://doi.org/10.1007/978-0-8176-4946-3\\_12](https://doi.org/10.1007/978-0-8176-4946-3_12)
- [5] Cristiani, E., Piccoli, B. and Tosin, A. (2011) Multiscale Modeling of Granular Flows with Application to Crowd Dynamics. *Multiscale Modeling & Simulation*, **9**, 155-182. <https://doi.org/10.1137/100797515>
- [6] Helbing, D., Johansson, A. and Al-Abideen, H.Z. (2007) Dynamics of Crowd Disasters: An Empirical Study. *Physical Review E*, **75**, Article ID: 046109. <https://doi.org/10.1103/PhysRevE.75.046109>
- [7] Helbing, D. and Molnár, P. (1995) Social Force Model for Pedestrian Dynamics. *Physical Review E*, **51**, 4282-4286. <https://doi.org/10.1103/PhysRevE.51.4282>
- [8] Helbing, D., Molnár, P., Farkas, I.J. and Bolay, K. (2001) Self-Organizing Pedestrian Movement. *Environment and Planning B: Planning and Design*, **28**, 361-383. <https://doi.org/10.1068/b2697>

- [9] Coscia, V. and Canavesio, C. (2008) First Order Macroscopic Modelling of Human Crowds. *Mathematical Models and Methods in Applied Sciences*, **18**, 1217-1247. <https://doi.org/10.1142/S0218202508003017>
- [10] Degond, P., Appert-Rolland, C., Pettré, J. and Theraulaz, G. (2013) Vision-Based Macroscopic Pedestrian Models. *Kinetic and Related Models*, **6**, 809-839. <https://doi.org/10.3934/krm.2013.6.809>
- [11] Hartmann, D. and Von Sivers, I. (2013) Structured First Order Conservation Models for Pedestrian Dynamics. *Networks and Heterogeneous Media*, **8**, 985-1007. <https://doi.org/10.3934/nhm.2013.8.985>
- [12] Henderson, L.F. (1974) On the Fluid Mechanic of Human Crowd Motion. *Transportation Research*, **8**, 509-515. [https://doi.org/10.1016/0041-1647\(74\)90027-6](https://doi.org/10.1016/0041-1647(74)90027-6)
- [13] Hoogendoorn, L.S. and Bovy, P.H.L. (2004) Dynamic User-Optimal Assignment in Continuous Time and Space. *Transportation Research Part B: Methodological*, **38**, 571-592. <https://doi.org/10.1016/j.trb.2002.12.001>
- [14] Hughes, R.L. (2002) A Continuum Theory for the Flow of Pedestrians, *Transportation Research Part B: Methodological*, **36**, 507-535. [https://doi.org/10.1016/S0191-2615\(01\)00015-7](https://doi.org/10.1016/S0191-2615(01)00015-7)
- [15] Hughes, R.L. (2003) The Flow of Human Crowds. *Annual Review of Fluid Mechanics*, **35**, 169-183. <https://doi.org/10.1146/annurev.fluid.35.101101.161136>
- [16] Maury, B., Roudneff-Chupin, A. and Stantambrogio, F. (2010) A Macroscopic Crowd Motion Model of Gradient Flow Type. *Mathematical Models and Methods in Applied Sciences*, **20**, 1787-1821. <https://doi.org/10.1142/S0218202510004799>
- [17] Piccoli, B. and Tosin, A. (2009) Pedestrian Flows in Bounded Domains with Obstacles. *Continuum Mechanics and Thermodynamics*, **21**, 85-107. <https://doi.org/10.1007/s00161-009-0100-x>
- [18] Piccoli, B. and Tosin, A. (2011) Time-Evolving Measures and Macroscopic Modeling of Pedestrian Flow. *Archive for Rational Mechanics and Analysis*, **199**, 707-738. <https://doi.org/10.1007/s00205-010-0366-y>
- [19] Agnelli, J.P., Colasuonno, F. and Knopoff, D. (2015) A Kinetic Theory Approach to the Dynamics of Crowd Evacuation from Bounded Domains. *Mathematical Models and Methods in Applied Sciences*, **25**, 109-129. <https://doi.org/10.1142/S0218202515500049>
- [20] Degond, P., Appert-Rolland, C., Moussaïd, M., Pettré, J. and Theraulaz, G. (2013) A Hierarchy of Heuristic-Based Models of Crowd Dynamics. *Journal of Statistical Physics*, **152**, 1033-1068. <https://doi.org/10.1007/s10955-013-0805-x>
- [21] Kim, D. and Quaini, A. (2019) A Kinetic Theory Approach to Model Pedestrian Dynamics in Bounded Domains with Obstacles. *Kinetic and Related Models*, **12**, 1273-1296. <https://doi.org/10.3934/krm.2019049>
- [22] Bellomo, N., Clarke, D., Gibelli, L., Townsend, P. and Vreugdenhil, B.J. (2016) Human Behaviours in Evacuation Crowd Dynamics: from Modeling to “Big Data” toward Crisis Management. *Physics of Life Reviews*, **18**, 1-21. <https://doi.org/10.1016/j.plrev.2016.05.014>
- [23] Haghani, M. and Sarvi, M. (2017) Social Dynamics in Emergency Evacuations: Disentangling Crowds Attraction and Repulsion Effects. *Physica A*, **475**, 24-34. <https://doi.org/10.1016/j.physa.2017.02.010>
- [24] Helbing, D. and Johansson, A. (2012) Pedestrian Crowd and Evacuation Dynamics. In: Meyers, R., Eds., *Encyclopedia of Complexity and System Science*, Springer, New York, 1-28. [https://doi.org/10.1007/978-3-642-27737-5\\_382-5](https://doi.org/10.1007/978-3-642-27737-5_382-5)

- [25] Ronchi, F., Nieto Uriz, F., Criel, X. and Reilly, P. (2016) Modelling Large-Scale Evacuation of Music Festivals. *Case Studies in Fire Safety*, **5**, 11-19. <https://doi.org/10.1016/j.csfs.2015.12.002>
- [26] Twarogowska, M., Goatin, P. and Duvigneau, R. (2014) Macroscopic Modeling and Simulations of Room Evacuation. *Applied Mathematical Modelling*, **38**, 5781-5795. <https://doi.org/10.1016/j.apm.2014.03.027>
- [27] Bellouquid, A., De Angelis, E. and Fermo, L. (2012) Towards the Modeling of Vehicular Traffic as a Complex System: A Kinetic Theory Approach. *Mathematical Models and Methods in Applied Sciences*, **22**, Article ID: 1140003. <https://doi.org/10.1142/S0218202511400033>
- [28] Fermo, L. and Tosin, A. (2013) A Fully-Discrete-State Kinetic Theory Approach to Modeling Vehicular Traffic. *SIAM Journal on Applied Mathematics*, **73**, 1533-1556. <https://doi.org/10.1137/120897110>
- [29] Bellomo, N. and Soler, J. (2012) On the Mathematical Theory of the Dynamics of Swarms Viewed As A Complex System. *Mathematical Models and Methods in Applied Sciences*, **22**, Article ID: 1140006. <https://doi.org/10.1142/S0218202511400069>
- [30] Knopoff, D. (2013) On the Modeling of Migration Phenomena on Small Networks. *Mathematical Models and Methods in Applied Sciences*, **23**, 541-563. <https://doi.org/10.1142/S0218202512500558>
- [31] Appert-Rolland, C., Degond, P. and Motsch, S. (2011) Two-Way Multi-Lane Traffic Model for Pedestrians in Corridors. *Networks and Heterogeneous Media*, **6**, 351-381. <https://doi.org/10.3934/nhm.2011.6.351>
- [32] Bellomo, N., Gibelli, L. and Outada, N. (2019) on the Interplay between Behavioral Dynamics and Social Interactions in Human Crowds. *Kinetic and Related Models*, **12**, 397-409. <https://doi.org/10.3934/krm.2019017>
- [33] Borsche, R., Klar, A., Kühn, S. and Meurer, A. (2014) Coupling Traffic Flow Networks to Pedestrian Motion. *Mathematical Models and Methods in Applied Sciences*, **24**, 359-380. <https://doi.org/10.1142/S0218202513400113>
- [34] Roggen, D., Wirz, M., Tröster, G. and Helbing, D. (2011) Recognition of Crowd Behavior from Mobile Sensors with Pattern Analysis and Graph Clustering Methods. *Networks and Heterogeneous Media*, **6**, 521-544. <https://doi.org/10.3934/nhm.2011.6.521>
- [35] Gibelli, L. and Bellomo, N. (Eds.) (2018) Crowd Dynamics, Volume 1: Theory, Models, and Safety Problems. Birkhäuser, Cham. <https://doi.org/10.1007/978-3-030-05129-7>
- [36] Gibelli, L. (Eds.) (2020) Crowd Dynamics, Volume 2: Theory, Models, and Applications. Birkhäuser, Cham. <https://doi.org/10.1007/978-3-030-50450-2>
- [37] Schadschneider, A. and Seyfried, A. (2011) Empirical Results for Pedestrian Dynamics and Their Implications for Modeling. *Networks and Heterogeneous Media*, **6**, 545-560. <https://doi.org/10.3934/nhm.2011.6.545>
- [38] De Angelis, E. (1999) Nonlinear Hydrodynamic Models of Traffic Flow Modelling and Mathematical Problems. *Mathematical and Computer Modelling*, **29**, 83-95. [https://doi.org/10.1016/S0895-7177\(99\)00064-3](https://doi.org/10.1016/S0895-7177(99)00064-3)
- [39] Holden, H., Karlsen, K., Lie, K. and Risebro, N. (2010) Splitting Methods for Partial Differential Equations with Rough Solutions: Analysis and Matlab Programs. EMS Series of Lectures in Mathematics, European Mathematical Society, Zürich. <https://doi.org/10.4171/078>